Case Study

Robust Strategy for Assessing the Costs of Urban Drainage System Designs under Climate Change Scenarios

Marcos Abilio Medeiros de Saboia[1]; Francisco de Assis de Souza Filho[2]; Fernanda Helfer[3]; and Larissa Zaira Rafael Rolim[4]

Abstract: Uncertainty inherent in precipitation predictions from general circulation model (GCMs) may lead urban drainage systems to be underdesigned (or overdesigned) in the future. This issue can be mitigated with the use of risk analysis models. In this study, a decision-making tool, developed based on six models (minimin, minimax, expected value, Hurwicz, Savage, and scenario-based multiobjective robust optimization), was used to select GCM/representative concentration pathways (RCP) scenarios that would lead to robust designs of an urban drainage system located in Fortaleza, Brazil. The implementation costs of the studied drainage system were estimated using runoff derived from rainfall predictions from six GCMs and two RCPs. After applying the proposed decision-making tool, three GCM/RCP scenarios were selected for yielding the most resilient and reliable designs. The range of feasible GCM/RCP scenarios reflects the level of optimism or pessimism held by a decision maker. We strongly recommend that this method be incorporated in urban drainage system design in order to help municipal planners make better decisions in view of climate change uncertainty. **DOI: 10.1061/(ASCE)WR.1943-5452.0001281.**

Author keywords: Climate change; General circulation models (GCMs); Urban drainage.

Introduction

Climate projections indicate that temperature increases will cause significant changes in the average annual precipitation of almost the entire planet (IPCC 2012). The atmosphere's capacity to retain water has increased in many regions due to increased average temperatures, causing more intense rainfall events. Almost all regions in the world have been experiencing the effects of climate change; countries located in low latitudes have a higher probability of being impacted by extreme events (Green 2016; Harrington et al. 2016). In northeast Brazil, located in a low-latitude region, total rainfall volume tends to decrease due to climate change, but there is a tendency toward more intense rainfall episodes (Phillip 2011; Fischer and Knutti 2015; Mishra et al. 2015; Prein et al. 2017; Marengo et al. 2017; Ragno et al. 2018).

Changes in concentrations of greenhouse gases may alter the balance of the global climate system. These perturbations are measured by radiative forcings (RFs) (IPCC 2007; Andrews et al. 2015). Possible representative concentration pathways (RCPs) have been created by the Intergovernmental Panel on Climate Change (IPCC) to represent different climate futures, all of which are considered possible depending on the amount of greenhouse gases emitted in the years to come (IPCC 2014). These pathways project the values of RFs in the future (up to 2100) based on possible changes in the agents that promote climate change (mainly CO_2) (Van Vuuren et al. 2011; Myhre et al. 2015). Four pathways were created for the future—RCP 2.6; RCP 4.5; RCP 6, and RCP 8.5 (IPCC 2012). RCP 8.5 is a scenario with little curbing of emissions, in which CO_2 concentrations continue to rise rapidly. RCP 6 is a lower-emission scenario, achieved by the application of some mitigation strategies and technologies. RCP 4.5 is associated with a low rate of greenhouse gas emissions and the use of a reasonable amount of political and environmental measures. RCP 2.6 is the most ambitious mitigation scenario, requiring stringent climate policies to limit emissions (Van Vuuren et al. 2011; Climate Changes in Australia 2019).

General circulation models (GCMs) can be used to estimate, with various levels of precision and accuracy, the future precipitation conditions of a given location based on possible RCPs (Schardong et al. 2015). They can predict changes in the earth's atmosphere caused by specific compounds that promote global warming, especially greenhouse gases.

Changes in the total precipitation volume and intensity, in turn, will have a strong effect on current and future urban drainage systems. Problems with stormwater drainage have been aggravated, mainly in large cities, due to several factors, such as type of land occupation, deforestation, paving, irregular construction, and climate change. Some of these factors contribute to a reduction of water infiltration in the soil, and consequently, to increasing the volume of surface runoff (Mota 2012; Thakali et al. 2016). Climate change, combined with obsolete urban infrastructure, is likely to cause more urban floods (Guo 2006; Mailhot and Duchesne 2010; Phillip et al. 2011). In addition, the financial repercussions of such changes are a challenge to be solved and, therefore, will be the main focus of this study, which proposes a decision-making tool for assessing urban drainage system costs under climate change conditions.

[1]Research Fellow, School of Engineering and Built Environment, Griffith Univ., Gold Coast, QLD 4222, Australia (corresponding author). Email: marcos_abilio@hotmail.com

[2]Professor, Dept. of Hydraulic and Environmental Engineering, Federal Univ. of Ceará, Fortaleza, Ceará 60455-900, Brazil. Email: assis@ufc.br

[3]Lecturer, School of Engineering and Built Environment, Griffith Univ., Gold Coast, QLD 4222, Australia. Email: f.helfer@griffith.edu.au

[4]Master's Student, Dept. of Hydraulic and Environmental Engineering, Federal Univ. of Ceará, Fortaleza, Ceará 60455-900, Brazil. Email: larissazairar@gmail.com

Note. This manuscript was submitted on December 22, 2019; approved on May 22, 2020; published online on August 27, 2020. Discussion period open until January 27, 2021; separate discussions must be submitted for individual papers. This paper is part of the ***Journal of Water Resources Planning and Management***, © ASCE, ISSN 0733-9496.

Climate change may affect maximum rainfall intensities, which are the main input parameters for designing urban drainage systems. Maximum rainfall intensities can be represented by intensity–duration–frequency (IDF) curves. IDF curves are used to describe the relationship between rainfall intensity, rainfall duration, and rainfall frequency. Such curves have a direct impact on the design of hydraulic systems and, consequently, on their implementation costs (Simonovic et al. 2016; Maurer et al. 2017; Sarhadi and Soulis 2017). Presently, IDF curves are calculated under a stationary risk concept (Guo 2006; Mailhot and Duchesne 2010); in other words, the curves are derived from observed precipitation records, and it is assumed that the precipitation patterns will remain the same in the future. However, IDF curves should be updated for the future by considering a nonstationary risk concept (Mailhot and Duchesne 2010), which could yield more robust hydraulic system designs due to more reliable rainfall predictions. One way to accomplish this is to use precipitation data provided by GCMs to update IDF curves so as to reflect emergent anomalies in extreme precipitation caused by climate change (Schardong et al. 2015; Sarhadi and Soulis 2017).

Some authors have conducted studies regarding the use of GCM data to update IDF curves, and some of these studies evaluated their impacts on hydrologic and hydraulic designs. Mirhosseini et al. (2013), for instance, used data from six combinations of global and regional models for updating IDF curves. The results showed that the precipitation patterns for Alabama are veering toward less intense rainfall for short rainfall durations (i.e., less than 4 h). Based on these results, they concluded that current standards and guidelines for designing drainage infrastructures based on short rainfall durations can continue to be applied well in the future. Hassanzadeh et al. (2014) used GCMs to create future IDF curves for the city of Saskatoon in Canada. The new IDF curves showed that an increase in the short-duration annual maximum precipitation (up to 6 h) is likely to occur in Saskatoon for small return periods (up to 10 years). Maurer et al. (2017) estimated changes in peak flow frequency based on output from several climate projections using historic and projected future streamflow simulations at 421 sites across the western US. Regarding changes in the peak flow return period, they concluded that, by the end of the 21st century, what is considered to be a 100-year event in the late 20th century can be expected to be approximately a 40-year event. If a lower greenhouse gas emission rate is followed, increases in flood frequency will be more modest or will occur later. Also, the authors recommended that regional planners incorporate projected peak flows into future hydrologic and hydraulic designs. In another example, Simonovic et al. (2016) analyzed precipitation data from 567 meteorological stations in Canada, using the web-based IDF_CC tool to generate future IDF curves. In this study, two precipitation events were analyzed; the first one was a short duration (2 h) event with a high frequency (5 years), which is frequently used for urban stormwater management applications, and the second one was a long duration (24 h) event with a low frequency (100 years), which is used in the management of flood risk in Canada. In both cases, the extreme precipitation values increased with an increase in the RCP number.

Previous studies have attempted to account for climatic uncertainties in urban drainage system designs using a variety of approaches. Maimone et al. (2019), for instance, used rainfall data from nine GCMs to generate future hourly rainfall time series for the design of stormwater drainage systems in the city of Philadelphia. Semadeni-Davies et al. (2008) used a regional circulation model to address the impacts of increased precipitation on the design of the urban drainage system of Helsingborg, Sweden. Despite numerous attempts to address climate change uncertainty in urban drainage system design using a multimodel ensemble approach, a method to deal with the uncertainty inherent in climate change prediction as well as with the level of optimism or pessimism held by the decision maker still seems to be missing and deserving of further investigation. Determining the impacts of climate change on maximum rainfall and, consequently, on urban drainage systems, is fundamental for stormwater management. In this context, many water resources decision makers aim to reach reliable results using multi-objective optimization while remaining robust to deviations from their results (Herman et al. 2015).

Table 1. Summary of the risk analysis models

Type	Model
Classic	Minimin
	Minimax
	Expected value
	Hurwicz
	Savage
Modern	SMORO (scenario-based multiobjective robust optimization)

The current study proposes a decision-making tool for selecting climate change scenarios that will provide economically viable solutions for urban drainage system design. This tool assesses drainage costs derived from rainfall intensities obtained from 12 different GCM/RCP scenarios and from one baseline (current) scenario. This assessment is based on the use of six risk analysis models (five classic models and one modern model, as specified in Table 1). Although this investigation was conducted in the city of Fortaleza, Brazil, as a case study, the methodology used is universal and transferrable and can be used elsewhere if rainfall projections for the future are available. It is hoped that this tool will help engineers to select specific GCM/RCP scenarios for updating IDF curves, which will certainly lead to more robust and resilient urban drainage system designs.

Methodology

Fig. 1 shows the framework of the proposed decision-making tool designed for this study. The first step of the approach is to extract daily maximum rainfall values from GCMs and daily and subdaily maximum rainfall values from a local rainfall gauge station. The next step is to perform statistical downscaling using the equidistant quantile matching method (EQMM) developed by Srivastav et al. (2014). In the third step, new, updated IDF curves are created based on GCM data, and information about the modeled basin (such as area, perimeter, length, and slope) is obtained. The next step involves using a computational model—the hydrologic engineering center hydrologic modeling system (HEC-HMS)—to model the rainfall–runoff process based on the new, updated IDF curves. The fifth step consists of calculating the implementation costs of each urban drainage system design based on the new, updated runoff amounts. In the last step, six risk analysis models are used to choose the most appropriate climate change scenarios. The details of these steps will be provided in the following sections.

Although the current study focused on the city of Fortaleza (the capital of the state of Ceará, Brazil), the proposed decision-making tool is replicable worldwide and can be applied in any urban catchment for which relevant data and information are available.

Study Area

The city of Fortaleza, the capital of the state of Ceará, Brazil, is situated in the Brazilian northeast; it is a costal city located at a

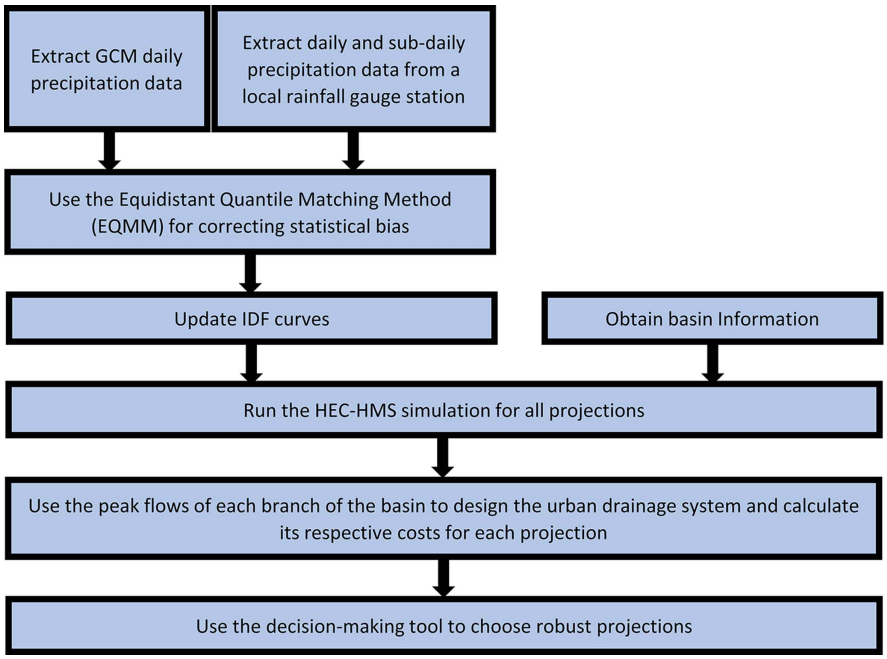

Fig. 1. Flowchart of the proposed methodology for choosing an appropriate climate change scenario.

low latitude (3.7° S). It has a total area of 313.14 km^2 and an average altitude of 16 m. It has a subhumid tropical climate, with a long-term average annual rainfall of 1,338 mm, and an average daily temperature ranging from 26°C to 28°C.

In Fortaleza, a large urban expansion occurred in recent decades; this expansion was not accompanied by a proper infrastructure planning. This disorderly growth has caused severe consequences to the city, including the deterioration of its urban drainage systems, which have caused many flooding events in recent years (Municipal Secretariat of Urbanism and Environment 2013).

The basin used in this study is called Riacho Tauape. The catchment area is approximately 3.5 km^2 and is in the south-central region of Fortaleza. The location of the area modeled is shown in Fig. 2; highlighted sections represent the drainage system layout suggested for the site.

Precipitation Data

Two sources of precipitation data were used in this study: a rainfall gauge station located in Fortaleza, and projections from GCMs.

The statistical analysis of the precipitation data from a rainfall gauge station, located in Fortaleza, was conducted through continuous records every 5 min from 1970 to 1999 (30 years). Maximum annual rainfall events were evaluated for durations of 5 min, 10 min, 15 min, 20 min, 25 min, 30 min, 1 h, 2 h, 6 h, 12 h, 18 h, and 24 h.

Daily precipitation data were also extracted from six GCMs for the RCP 4.5 and RCP 8.5 emission pathways. These two RCP scenarios were used in the simulation, because in the first scenario, it is assumed that the carbon dioxide emission levels will be maintained, whereas in the second scenario, it is assumed that carbon dioxide emission levels will increase drastically (Kim et al. 2015).Two timeframes were extracted from the GCMs: 1970 to 1999 and 2070 to 2099. Table 2 shows the GCMs used in this paper. Silveira et al. (2013) evaluated these coupled model intercomparison project phase 5 (CMIP5) models with regard to their representation of patterns of precipitation over northeast Brazil. Their study showed that these models represent the region's precipitation patterns with high accuracy. Silveira et al. (2016) also analyzed precipitation projections in the São Francisco river basin, which is also in northeast Brazil, and the results showed that the CMIP5 projections were reliable for that region.

Downscaling

General and regional circulation models have spatial resolutions incompatible with the size of a river basin. Thus, it was necessary to find a link between the data obtained using these models and their equivalents at a higher resolution (closer to reality). One of the techniques used to make this connection is called spatial downscaling. There are two types of downscaling: dynamic and statistical. Dynamic downscaling is based on limited area models or using extremely high-resolution circulation models to simulate local conditions (Li et al. 2010; Maurer and Hidalgo 2008). Statistical downscaling is based on transfer functions used to relate the global data to study sites (Schardong et al. 2015; Simonovic et al. 2016).

In this study, statistical downscaling of precipitation data was performed using EQMM to correct the statistical bias present in the samples generated by the GCMs. Srivastav et al. (2014) found that this method can incorporate the changes in the distributional characteristics of the GCM data between the baseline period and the future period. Furthermore, it is simple to adopt and computationally efficient. EQMM is based on two main assumptions. The first is that the data referring to the maximum daily rainfall generated by the GCM and the subdaily maximum rainfalls extracted from the observed data should be correlated. The second assumption refers to the accomplishment of temporal downscaling relating the maximum daily rainfalls generated by the GCM (historical series) and the maximum daily rainfalls relative to the future projections of the GCM (Schardong et al. 2015). Thus, the relationship between observed historical data and the data obtained by the GCM (bias correction) must first be established so that future rainfall timeseries can be estimated.

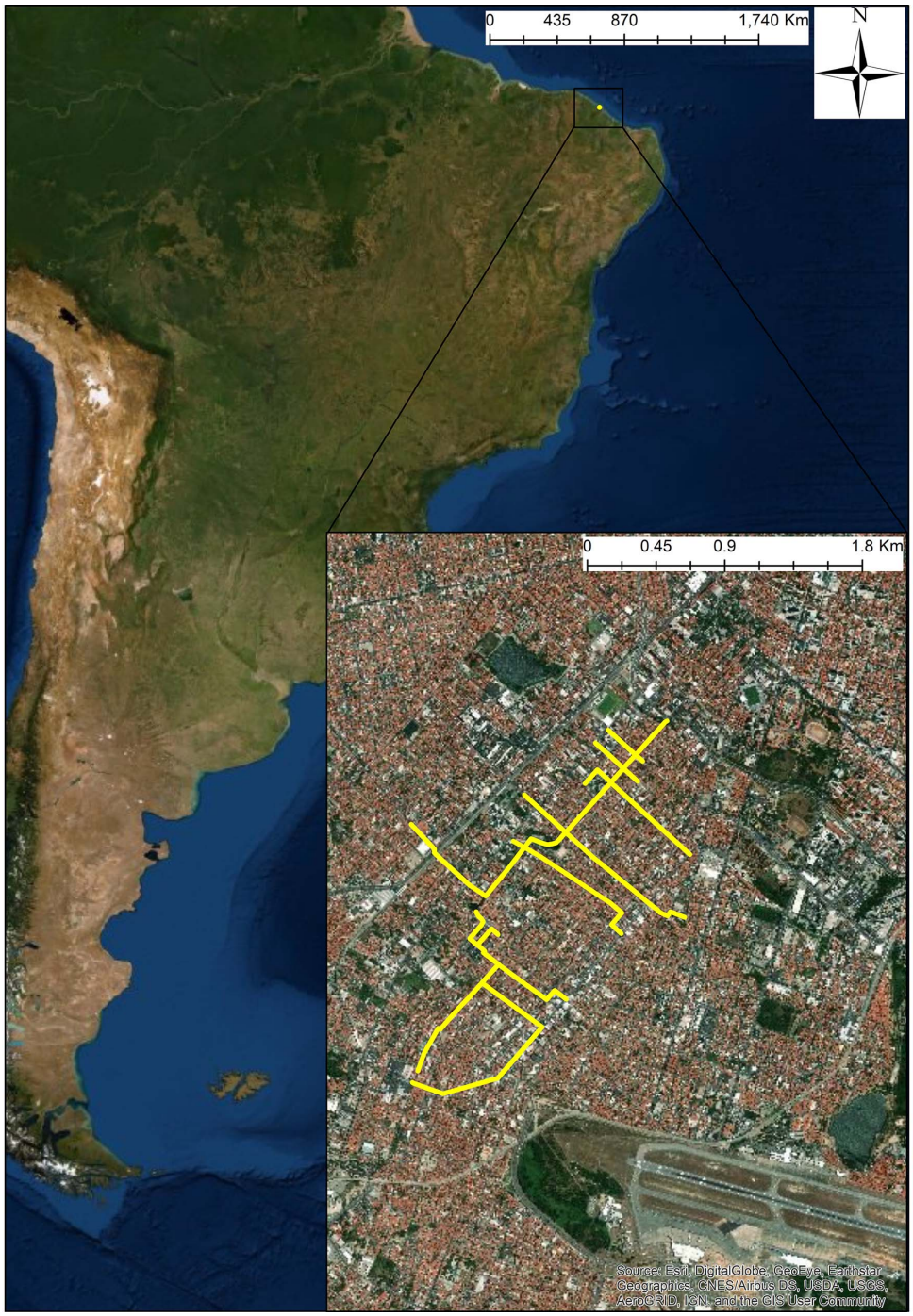

Fig. 2. Location of the modeled subbasin in Fortaleza, Ceara, Brazil. The lines represent the various drainage branches modeled in the current study. (Source: Esri, DigitalGlobe, GeoEye, Earthstar Geographics, CNES/Airbus DS, USDA, USGS, AeroGrid, IGN, and the GIS User Community.)

Table 2. GCMs used in this study

Model	Research center	Spatial grid resolution (in degrees)
BCC_CSM1	Beijing Climate Center, China Meteorological Administration	2.8×2.8
CANESM2	Canadian Centre for Climate Modeling and Analysis	2.8×2.8
CCSM4	National Center for Atmospheric Research, US	1.25×0.94
CESM1-CAM5	National Center for Atmospheric Research, US	1.25×0.94
INMCM4	Institute for Numerical Mathematics, Russia	2.00×1.50
MIROC5	Japan Agency for Marine-Earth Science and Technology	1.4×1.41

This method can be summarized by the following three steps:

1. Establish a statistical relationship between the annual maximum precipitation from the GCM and field data for the same period.
2. Establish a statistical relationship between the annual maximum precipitation from the GCM for the base period and the future period to be analyzed.
3. Establish a statistical relationship between Steps 1 and 2 with the intention of updating the IDF curves for the future.

GCM data were provided on a daily basis; however, sub-daily rainfall (15 min, 30 min, 1 h, and so forth) are needed to build IDF equations. To overcome this issue, the method proposed by Schardong et al. (2015) was used to disaggregate the daily rainfall data. In this method, the disaggregation is performed by considering cumulative distribution functions (CDFs). First, the annual daily maximum GCM rainfall from 1970 to 1999 was calculated. Then, a probability distribution function was fitted to these data. The distribution of extreme values of type I, the Gumbel distribution, was used, because it is widely used in the analysis of hydrological events. To verify the goodness of fit of the Gumbel distribution to the data, the Kolmogorov-Smirnov (KS) test was applied to verify adherence. The KS test can be calculated based on the largest difference between empirical and theoretical CDFs. Using a test significance level of 0.10, the KS test showed that the Gumbel distribution fitted to all series of maximum precipitation projections generated by the six GCMs. The maximum rainfall values were calculated for the following return periods: 5, 10, 15, 20, 25, 50, and 100 years. The daily precipitations were disaggregated using EQMM in order to generate rainfall of 2 h, 1 h, 30 min, 25 min, 20 min, 15 min, 10 min, and 5 min. Then, the new IDF curves were created based on these data.

Rainfall–Runoff Modeling

The computational model HEC-HMS was used to simulate the rainfall–runoff process in the basin shown in Fig. 2. This program has been applied in various basins worldwide and in a variety of studies, such as flow forecasting, urban drainage, and flood damage reduction studies (e.g., Scharffenberg 2013; Chu and Steinman 2009; Anderson et al. 2002; and De Silva et al. 2014).

In the HEC-HMS model, the surface runoff of the basin was computed assuming precipitation uniformly distributed over space. The hyetographs adopted were based on the Fortaleza's IDF equation [Autarquia Metropolitana de Fortaleza (AUMEF)] and on the 12 new equations built from GCM/RCP scenarios, for a total of 13 scenarios. Then, precipitations of 5- and 15-min and 1-, 2-, 3- and 6-h durations were calculated, based on a 50-year return period. In this study, a return period of 50 years was considered because this is the recommended practice in urban drainage design (Tucci 1993). The Soil Conservation Service (SCS) method was used in the HEC-HMS model for runoff volume and peak discharge estimation. This method has been widely used in similar studies (e.g., Yu 2012; Steenhuis et al. 1995; and Williams et al. 2012). The SCS method requires basin parameters (such as area, perimeter, length, and slope), precipitation, and the curve number (CN). The CN depends on a basin's soil and cover conditions (USDA 1986). For this study, land use remained unchanged in the future simulations in order to analyze the effects of climate change alone. The flowchart in Fig. 3 illustrates the rainfall–runoff modeling procedure.

Implementation Costs of the Urban Drainage System

Implementation costs of the urban drainage system were calculated based on the 12 GCM/RCP scenarios and a baseline scenario based on AUMEF (the official IDF equation for Fortaleza), for a total of 13 possible scenarios. After the rainfall–runoff modeling, the peak flows of each branch of the basin were obtained. Based on the peak flows of each branch and considering the 13 scenarios, the implementation costs of the urban drainage system were calculated. Implementation costs are closely related to the diameter of the underground stormwater pipes; that is, the more intense the rainfall, the higher the peak flow and the implementation costs.

The total drainage cost for each scenario included underground pipes (except the main open canal, which was already built), excavation and backfill services, the supplying and laying of concrete pipes, and the installation of gutters. Costs were based on prices on an important Brazilian reference cost table (Caixa Econômica Federal 2020), the National System of Costs Survey and Civil Construction Indices of September 2015 (SINAPI).

In view of the variety of possible scenarios for the implementation costs of the drainage system and the immense uncertainties with regard to how the climate will behave in the future, a decision-making tool for developing a robust urban drainage system design was applied, considering the effects of climate change. It was considered that all 12 GCM/RCP scenarios and the current scenario would have the same probability of occurring. This assumption was

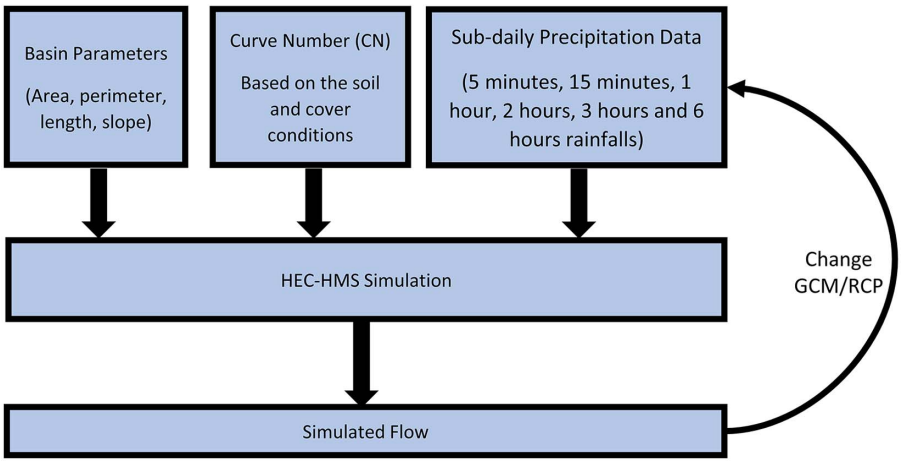

Fig. 3. Flowchart of the rainfall–runoff simulation. Basin parameters, curve number, and time of simulation were used as fixed parameters. In each simulation, the precipitation was based on the chosen scenario.

made because it is not known which scenario has the greatest chance of occurring in the future. In the current analysis, six risk analysis models were used; they will be described in the following section.

A cost matrix for the implementation of each scenario was developed based on the following reasoning. If, in the future, the existing design infrastructure (which is currently in use and has a cost = C_1) has enough capacity to operate under the future scenario, then no additional capital costs are incurred. Otherwise, if a certain future scenario occurs and the existing urban drainage system (with a cost = C_1) is underdesigned for that scenario, then additional infrastructure costs will be required. In this case, an additional cost for implementing this new design must be considered. Therefore, there will be a deployment cost of C_2 in addition to C_1 (i.e., total cost $= C_1 + C_2$). It is important to note that it is assumed that municipal planners, will have knowledge regarding the updated IDF curves in the future.

The cost matrix was constructed as shown in Table 3. It was also necessary to obtain a regret cost matrix (Table 4), in which each cell corresponds to the value of the difference between the total cost and the lowest implementation cost of each scenario, as per Table 3.

Risk Analysis Models

After the calculation of the cost matrix (Table 3) and the regret matrix (Table 4), the next step was to identify which urban drainage system design, based on the different GCM/RCP scenarios or the baseline scenario and considering their implementation costs, should be chosen considering the results of the following risk analysis models: expected value, minimin, minimax, Hurwicz, Savage, and scenario-based multiobjective robust optimization (SMORO).

These risk analysis models cover a wide range of pessimistic and optimistic urban drainage system designs. In other words, there is a direct relation between the degree of conservativeness of the decision maker and the choice of model. The risk analysis models used in this study and their formulations are described in the following subsections.

Expected Value

The expected value of a variable X can be obtained by weighting by p_x the probability mass function [Eq. (1) for discrete variables] of possible values of the random variable

$$E[X] = \sum_{all x_i} x_i p_x(x_i) \tag{1}$$

where $E[X]$ = expected value based on a set of values of the variable x. In this case, x is related to the regret cost.

The expected value risk analysis model can be used to associate a probability of occurrence to a specific scenario. In this study, the term *scenario* is used to refer to any of the 12 combinations of GCMs and RCPs, plus the baseline (current) scenario. It is important to note that all combinations of GCMs and RCPs as well as the baseline (current) scenario were treated as being equally likely.

The result of the expected value model is given by the choice of the lowest average value of the costs implemented by each scenario, that is, the lowest average value of each row in Table 3.

Minimin

In this risk analysis model, a more optimistic consideration of the future scenarios is adopted, and it is assumed that the least

Table 3. Cost matrix

	Future design			
Selected design	1	2	...	13
1	Total cost $= C_1$	If $(C_2 \le C_1)$ Total cost $= C_1$ If $(C_2 > C_1)$ Total cost $= C_1 + C_2$	...	If $(C_{13} \le C_1)$ Total cost $= C_1$ If $(C_{13} > C_1)$ Total cost $= C_1 + C_{13}$
2	If $(C_1 \le C_2)$ Total cost $= C_2$ If $(C_1 > C_2)$ Total cost $= C_2 + C_1$	Total cost $= C_2$	...	If $(C_{13} \le C_2)$ Total cost $= C_2$ If $(C_{13} > C_1)$ Total cost $= C_2 + C_{13}$
...				
13	If $(C_1 \le C_{13})$ Total cost $= C_{13}$ If $(C_1 > C_{13})$ Total cost $= C_{13} + C_1$	If $(C_2 \le C_n)$ Total cost $= C_1$ If $(C_2 > C_1)$ Total cost $= C_n + C_2$	...	Total cost $= C_{13}$
Minimum cost	Lowest cost of Column 1	Lowest cost of Column 2	...	Lowest cost of Column 13

Table 4. Regret cost matrix

	Future design			
Selected design	1	2	...	13
1	Regret = total cost C_1 − lowest cost of Table 3 Column 1	Regret = total cost C_1 − lowest cost of Table 3 Column 2	...	Regret = total cost C_1 − lowest cost of Table 3 Column 13
2	Regret = total cost C_2 − lowest cost of Table 3 Column 1	Regret = total cost C_2 − lowest cost of Table 3 Column 2	...	Regret = total cost C_2 − lowest cost of Table 3 Column 13
...				
13	Regret total cost C_{13} − lowest cost of Table 3 Column 1	Regret total cost C_{13} − lowest cost of Table 3 Column 2	...	Regret total cost C_{13} − lowest cost of Table 3 Column 13

expensive scenario will occur (the best-case scenario). The decision to be made is based on cost minimization, trying to reduce implementation cost for each scenario at maximum.

The decision maker wants to minimize the implementation cost of each scenario and ignores the possibility of extreme implementation costs (Mavromatidis et al. 2018). This suggests that the decision maker should examine the minimum implementation cost of the scenarios and choose the scenario with the lowest cost (Lau et al. 2010).

In this study, the minimin risk analysis model was calculated by obtaining the minimum value among the lowest values of each row in Table 3.

Minimax

According to Espinet et al. (2017), the minimax risk analysis model is closely related to a risk-averse attitude. This risk analysis model assumes that the most pessimistic climate change scenario will occur. Because considering that the results are based on cost minimization, the decision maker should try to minimize the maximum costs that may occur (Andrade 1989). This model should provide one of the most expensive implementation costs due to its high degree of conservativeness.

In this study, the minimax risk analysis model was calculated by obtaining the minimum value among the maximum values of each row in Table 3.

Hurwicz

According to Mavromatidis et al. (2018), this risk analysis model admits that decision makers, in general, are not extremely pessimistic or optimistic and provides a rule of decision making between these two limits. If the decision maker is willing to demonstrate some degree of optimism (or pessimism) in the choice of scenarios, the Hurwicz risk analysis model can be used.

The Hurwicz risk analysis model seeks to weigh optimistic and pessimistic views through a factor called the coefficient of optimism (Lau et al. 2010). Given a coefficient of optimism α, the value associated with each scenario is calculated from Eq. (2)

$$H(A_i) = \alpha[\max(A_i)] + (1 - \alpha)[\min(A_i)] \tag{2}$$

where $H(A_i)$ = associated value of the Hurwicz risk analysis model; α = probability of the most optimistic scenario; $1 - \alpha$ = probability of the most pessimistic scenario; $\max(A_i)$ = maximum expected value; and $\min(A_i)$ = minimum expected value. The greater the optimism, the closer the solution to the lower-cost scenario.

Based on Eq. (2), this risk analysis model establishes a linear relation between the maximum and minimum expected values. This risk analysis model establishes a set of optimal solutions assigned to each degree (%) of optimism regarding total deployment costs. The results may vary from the worst-case scenario and best-case scenario depending on the degree of optimism of the decision maker.

In this case, using the Hurwicz risk analysis model, there are a range of scenarios that can be selected.

Savage

The Savage risk analysis model, or the risk analysis model of less regret, is based on the principle that the scenario that generates the least regret must be chosen. In other words, the chosen scenario must be the one in which the maximum risk is minimized in the most optimistic conditions (Khodakivskyia et al. 2019), that is, in which there is the smallest difference between a given scenario and the worst scenario studied.

This risk analysis model is a variant of the minimax; it calculates the minimization of the maximum regret corresponding to each possible scenario (Kassa 2017). Regret is calculated as the difference between the obtained result and the result that would be obtained if the best scenario were chosen (Bekman and Costa Neto 1980).

For the calculation of the most suitable scenario using the Savage risk analysis model, which is based on the regret matrix, the decision maker should calculate the maximum regret for each scenario. Then, the smallest one among them is chosen.

In this study, the Savage risk analysis model was calculated by obtaining the minimum value among the maximum values of each row in Table 4.

SMORO

According to Kang and Lansey (2013), a primary goal of scenario planning is to allow flexibility and add robustness to a system so that it can respond to a range of uncertain scenarios at a reasonable cost. The SMORO risk analysis model considers multiple possible scenarios in order to find the most robust one. Two objective functions to be minimized are used, namely, F_1, which represents the expected cost, and F_2, which represents the standard deviation of costs through the scenarios

$$F_1 = E[C(X, \Delta X|\omega)] = \sum_{k=1}^{N} Pr_k \times C(X, \Delta X_k|\omega_k) \tag{3}$$

$$F_2 = \left\{ \sum_{k=1}^{N} Pr_k [F_1 - C(X, \Delta X_k|\omega_k)]^2 \right\}^{\frac{1}{2}} \tag{4}$$

$$\text{Subject to } G(X, \Delta X^k|\omega^k) > 0, \quad \forall\ k, \quad k = 1, \ldots, N \tag{5}$$

where X and ΔX = initial decision and expansion vectors of the system, respectively; and G = general set of constraints on X that include the system parameters, ω

$$C(X, \Delta X|\omega) = C(X|\omega) + C^S(\Delta X|\omega) \tag{6}$$

where $C(X|\omega)$ = initial cost of implementation of a scenario, given certain preestablished conditions. The equation $C^S(\Delta X|\omega)$ represents the additional cost of adapting a design to change ΔX in the initially planned scenario.

The variable Pr_k represents the probability of occurrence of a certain planned scenario k (they were considered equally likely), and N represents the total number of considered scenarios. The cost parameters of each scenario, based on the precipitation patterns, are represented by ω.

When the main goal is to minimize costs while also minimizing risks as defined by standard deviation, this methodology is used. As the most updated risk analysis model to be included in the analysis, SMORO can provide a set of optimal solutions, based on the minimization of two cost functions. The first is based on the average cost of each scenario, and the second refers to the minimization of standard deviations through the scenarios. Therefore, this set of optimal solutions can provide a wide range of robust solutions; the most suitable one can be chosen based on the degree of conservativeness of the decision maker.

Results

In this section, the updated IDF curves based on the GCM projections (RCP 4.5 and 8.5) are assessed and compared to the AUMEF

curve. Next, the implementation costs of the urban drainage system based on each of these updated IDF curves are quantified. Last, the results of the proposed decision-making tool are discussed.

IDF Curves under Climate Change Scenarios

In this study, new IDF curves were developed for the city of Fortaleza for future scenarios. The projected future IDF curves were compared to current curves from the AUMEF equation in order to identify possible changes in patterns of intense rainfall. The results for a 50-year return period are summarized in Fig. 4.

The Beijing climate center climate system model version 1.1 (BCC_CSM1) has one of the lowest spatial resolutions of the models analyzed (approximately 2.8° × 2.8°). Based on the analysis of the results of the BCC_CSM1 model [Fig. 4(a)], the projected curves for the two emission pathways (RCP 4.5 and RCP 8.5) presented rain intensities much lower than the rainfall intensities from the AUMEF curve. The average decrease in rainfall intensity was 49% for the RCP 4.5 pathway and 41% for the RCP 8.5 pathway.

The second generation Canadian earth system model (CANESM2) has one of the lowest spatial resolutions among the models used (2.8° × 2.8°). Under the RCP 4.5 pathway, there is indication that there will be a decrease in the intensity of maximum rainfall, especially in rainfall events lasting less than 1 h. However, the RCP 8.5 trajectory points to an increase in maximum rainfall intensity, except for short-duration rainfall events (approximately 5 min) and remains close to the durations indicated by the AUMEF curve. The results point to an average decrease in rainfall intensity of 23% for the RCP 4.5 pathway and of 18% for the RCP 8.5 pathway [Fig. 4(b)].

The community earth system model version 1 that includes the community atmospheric model version 5 (CESM1-CAM5) (spatial resolution of 1.25° × 0.94°) was the one that presented the most extreme values of rainfall among the models analyzed [Fig. 4(c)]. Under the RCP 4.5 emission pathway, this model showed increases in maximum rainfall intensities, presenting an average increase of 30% compared to the AUMEF equation. Under the RCP 8.5 pathway, this model had an average increase of 219% compared to the rainfall intensities estimated by the AUMEF curve.

The community climate system model version 4 (CCSM4) (spatial resolution of 1.25° × 0.94°) showed results with an increase in precipitation compared to the AUMEF IDF curve [Fig. 4(d)].

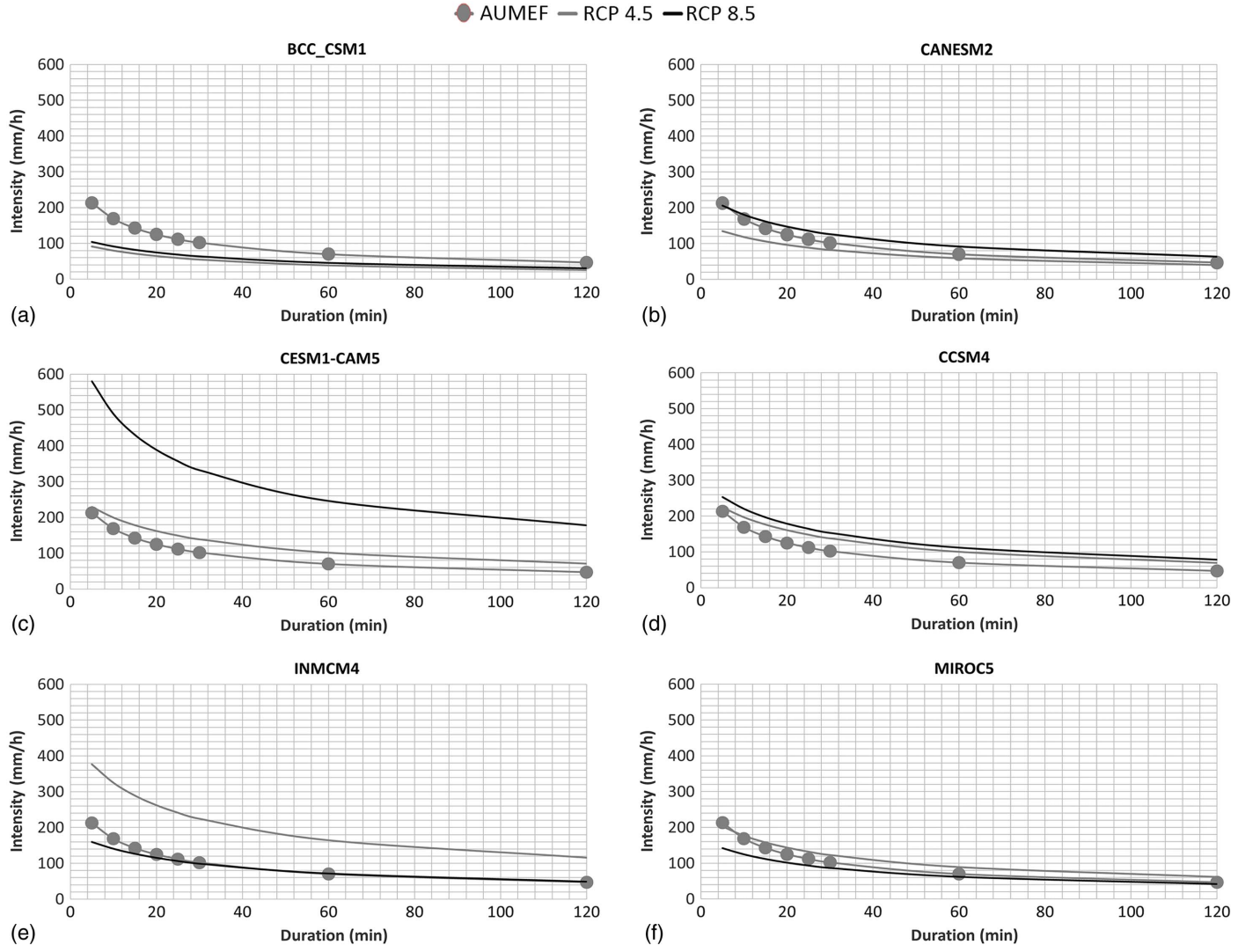

Fig. 4. IDF curves of the official equation of Fortaleza (AUMEF) and IDF curves derived for climate change scenarios (combinations of GCMs and RCPs) for a return period of 50 years: (a) BCC_CSM1; (b) CANESM2; (c) CESM1-CAM5; (d) CCSM4; (e) INMCM4; and (f) MIROC5. The gray line with circles indicates the AUMEF equation; the gray line indicates RCP 4.5; and the black line indicates RCP 8.5.

J. Water Resour. Plann. Manage., 2020, 146(11): 05020022

As seen in Fig. 4(d), the curves for the two pathways (RCP 4.5 and 8.5) had average increases of 29% and 44%, respectively.

The Institute of Numerical Mathematics Climate Model version 4 (INMCM4) has a spatial resolution of 2.00° × 1.50°, slightly less precise than the CESM1-CAM5 and CCSM4 models. The curve for the RCP 4.5 pathway had an average increase in rainfall intensity of 112%. The curves for the RCP 8.5 pathway and the AUMEF equation, in turn, practically overlapped for rainfall events with durations above 25 min [Fig. 4(e)].

For the model for interdisciplinary research on climate version 5 (MIROC5) (spatial resolution of 1.4° × 1.41°), the IDF curve based on the RCP 4.5 pathway had an average increase in rainfall intensity of 18% for rainfall events with durations above 10 min. The IDF curve based on the RCP 8.5 pathway had the lowest values of intensities for any rainfall duration analyzed. For this scenario, the average decrease in rainfall intensity was 19%. However, the longer the rainfall duration, the more the curve equated to the AUMEF curve; this was especially true for rainfall lasting longer than 1 h [Fig. 4(f)].

For the RCP 4.5 emission pathway, four GCMs projected an increase in rainfall intensities in the future. For the RCP 8.5 pathway, only three models projected an increase in rainfall intensities relative to the AUMEF curve. This suggests that there is a great deal of uncertainty regarding the GCM precipitation scenarios.

Implementation Costs for Each Scenario

The implementation costs of the urban drainage system were based on the results from the use of the official Fortaleza IDF equation (AUMEF) and the IDF equations projected for the future from the six GCMs for the two RCPs (4.5 and 8.5), shown previously in Fig. 4. Table 5 shows that there is a great variation in costs across the different equations used, demonstrating the wide range of uncertainty inherent in current model predictions of climate change. The RCP 4.5 pathway presents the most optimistic system infrastructure cost, with an implementation cost of USD 0.9 million, as well as the most pessimistic cost, with an implementation cost of USD 4.7 million. The calculated average cost of the models under RCP 4.5 was USD 2.8 million. The RCP 8.5 emission pathway yielded implementation costs of USD 1.0 million and USD 6.0 million, respectively, for the most optimistic and most pessimistic outcomes. The average value of implementation cost calculated for the RCP 8.5 pathway was USD 3.0 million, slightly higher than the average for the RCP 4.5 pathway.

Table 5. Drainage system implementation costs (in millions of US dollars) based on each scenario

Scenario	Implementation costs
AUMEF (current climate)	USD 1.7
BCC_CSM1/RCP 4.5	USD 0.9
CANESM2/RCP 4.5	USD 1.5
CCSM4/RCP 4.5	USD 3.5
CESM1-CAM5/RCP 4.5	USD 3.5
INMCM4/RCP 4.5	USD 4.7
MIROC5/RCP 4.5	USD 3.0
BCC_CSM1/RCP 8.5	USD 1.0
CANESM2/RCP 8.5	USD 3.0
CCSM4/RCP 8.5	USD 4.1
CESM1-CAM5/RCP 8.5	USD 6.0
INMCM4/RCP 8.5	USD 2.2
MIROC5/RCP 8.5	USD 1.5

Note: The authors used the BRA/USD currency exchange rate (3.86) from June 6, 2019.

Urban Drainage System Design under Climate Change Conditions

To carry out the design of the drainage system, the cost matrix (Table 3) was calculated. Next, the regret matrix (Table 4) was calculated so that the desired decision-making tool could be applied. Table 6 shows the chosen scenarios based on the expected value, minimin, minimax and Savage risk analysis models.

With regard to the expected value model, the BCC_CSM1/RCP 4.5 scenario had the lowest total cost among the expected values for each scenario, with a value of USD 3.6 million.

In order to determine the most suitable scenario using the minimin model, the lowest cost in the set of costs was selected. This was USD 0.9 million from the data generated by the BCC_CSM1/RCP 4.5 scenario.

For the minimax model, the lowest cost in the set of costs estimated for each of the scenarios studied was chosen; this was USD 6.0 million, based on the CESM1-CAM5/RCP 8.5 scenario.

For the Savage model, the lowest implementation cost was achieved with the BCC_CSM1/RCP 4.5 scenario, a value of USD 0.9 million. The data were analyzed on the regret matrix, choosing the scenario that represented the lowest of the set of maximum costs of regret of implementation of the scenarios.

Results were also obtained using the Hurwicz model, which is based on decision-making being contingent on the degree of optimism. It is important to remember that the CESM1-CAM5/RCP 8.5 scenario was the only scenario that was not sensitive to the degree of optimism, because it presents the most expensive implementation cost; even if another scenario occurs, the system will be overdesigned and no changes will need to be made. Using a degree of optimism of up to 14.43%, the CESM1-CAM5/RCP 8.5 scenario should be used. However, if optimism is estimated above this value, the BCC_CSM1/RCP 4.5 scenario should be used. A summary of these scenarios can be seen in Fig. 5.

The last risk analysis model analyzed, SMORO, provided a set of optimal solutions based on the minimization of expected average costs ($F1$) and deviations ($F2$) (Table 7). The CANESM2/RCP 4.5 scenario was chosen because it yields one of the most resilient and appropriate solutions (Fig. 6).

Based on the results from the risk analysis models, the selected design alternatives will result in good performance, considering the uncertainty inherent in climate change.

Table 6. Decision making based on the expected value, minimin, minimax, and Savage risk analysis models (in millions of US dollars)

	Risk analysis models			
Scenario	Expected value	Minimin	Minimax	*Savage*
AUMEF	USD 4.0	USD 1.7	USD 7.7	USD 1.7
BCC_CSM1/RCP 4.5	USD 3.6	USD 0.9	USD 6.8	USD 0.9
BCC_CSM1/RCP 8.5	USD 3.7	USD 1.0	USD 7.0	USD 1.0
CANESM2/RCP 4.5	USD 4.0	USD 1.5	USD 7.5	USD 1.5
CANESM2/RCP 8.5	USD 4.7	USD 3.0	USD 8.9	USD 3.0
CCSM4/RCP 4.5	USD 4.6	USD 3.5	USD 9.4	USD 3.5
CCSM4/RCP 8.5	USD 4.9	USD 4.1	USD 10.0	USD 4.1
CESM1-CAM5/RCP 4.5	USD 4.6	USD 3.5	USD 9.4	USD 3.5
CESM1-CAM5/RCP 8.5	USD 6.0	USD 6.0	USD 6.0	USD 5.1
INMCM4/RCP 4.5	USD 5.2	USD 4.7	USD 10.7	USD 4.7
INMCM4/RCP 8.5	USD 4.4	USD 2.2	USD 8.2	USD 2.2
MIROC5/RCP 4.5	USD 4.7	USD 3.0	USD 8.9	USD 3.0
MIROC5/RCP 8.5	USD 3.9	USD 1.5	USD 7.5	USD 1.5
Minimum Cost	USD 3.6	USD 0.9	USD 6.0	USD 0.9

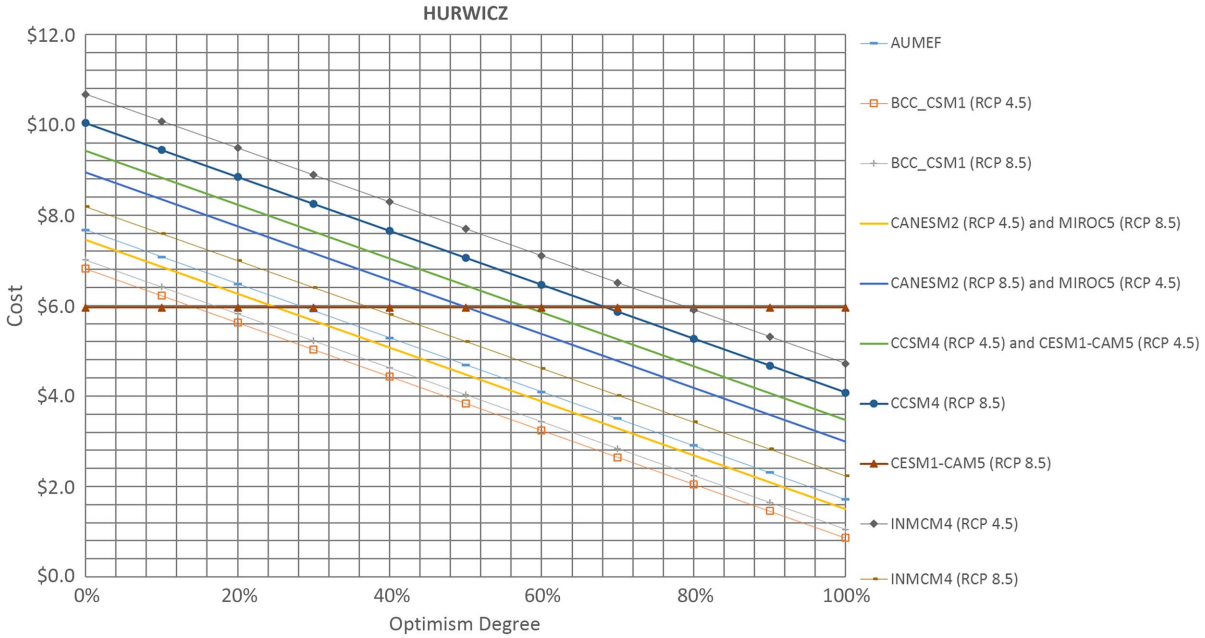

Fig. 5. Decision making under the Hurwicz risk analysis model for the 12 GCM/RCP scenarios and the baseline scenario (AUMEF curve). The expected cost of each scenario was based on the degree of optimism. Values are in millions of US dollars.

Table 7. Decision-making under SMORO risk analysis model (in millions of US dollars)

	Minimized functions	
Scenario	$F1$	$F2$
AUMEF	USD 4.0	USD 2.0
BCC_CSM1/RCP 4.5	USD 3.6	USD 1.6
BCC_CSM1/RCP 8.5	USD 3.7	USD 1.7
CANESM2/RCP 4.5	USD 4.0	USD 1.8
CANESM2/RCP 8.5	USD 4.7	USD 2.2
CCSM4/RCP 4.5	USD 4.6	USD 2.1
CCSM4/RCP 8.5	USD 4.9	USD 1.9
CESM1-CAM5/RCP 4.5	USD 4.6	USD 2.1
CESM1-CAM5/RCP 8.5	USD 6.0	USD 0.0
INMCM4/RCP 4.5	USD 5.2	USD 1.6
INMCM4/RCP 8.5	USD 4.4	USD 2.1
MIROC5/RCP 4.5	USD 4.7	USD 2.2
MIROC5/RCP 8.5	USD 3.9	USD 1.9

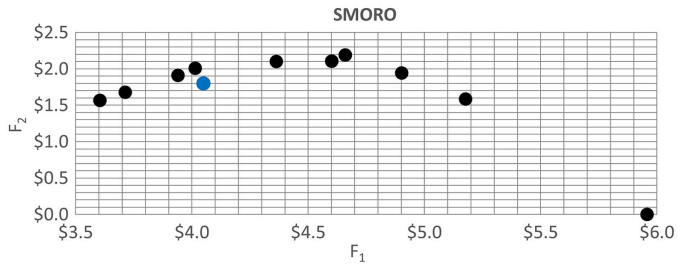

Fig. 6. Decision making under the SMORO risk analysis model for the 12 GCM/RCP scenarios and the baseline scenario (AUMEF curve). The variables F_1 and F_2 represent the expected cost and the standard deviation of costs, respectively. Values are in millions of US dollars. The chosen scenario is indicated by a gray circle.

Table 8. Scenarios selected for each of the risk analysis models (except SMORO)

Risk analysis model	Selected scenario
Expected value	BCC_CSM1/RCP 4.5
Minimin	BCC_CSM1/RCP 4.5
Minimax	CESM1-CAM5/RCP 8.5
Savage	BCC_CSM1/RCP 4.5
Hurwicz (optimism up to 14.43%)	CESM1-CAM5/RCP 8.5
Hurwicz (optimism above 14.43%)	BCC_CSM1/RCP 4.5

Table 8 presents a summary of the chosen GCM/RCP scenarios based on the risk analysis models used (not including SMORO).

Conclusions

This study proposed an approach to take into consideration uncertainty caused by climate change in urban drainage system design. The proposed approach can be applied in long-term planning of water resources infrastructures. The motivation for this study was the fact that costs of infrastructure play an important role in the decision making involved in water resources planning.

In Fortaleza, the city in which this study was conducted, uncertainty inherent in climate change is still not fully considered in current design projects. The proposed methodology generated new IDF curves based on climate change scenarios; the urban drainage system costs of each scenario were evaluated using five classic and one modern risk analysis models.

The IDF equation currently used in Fortaleza was developed based on rainfall data from 1928 to 1975. Hence, this equation does not reflect expected precipitation changes in the future. As presented in this study, there is a range of possibilities for future IDF curves, based on climate model predictions for precipitation, reflecting the

J. Water Resour. Plann. Manage., 2020, 146(11): 05020022

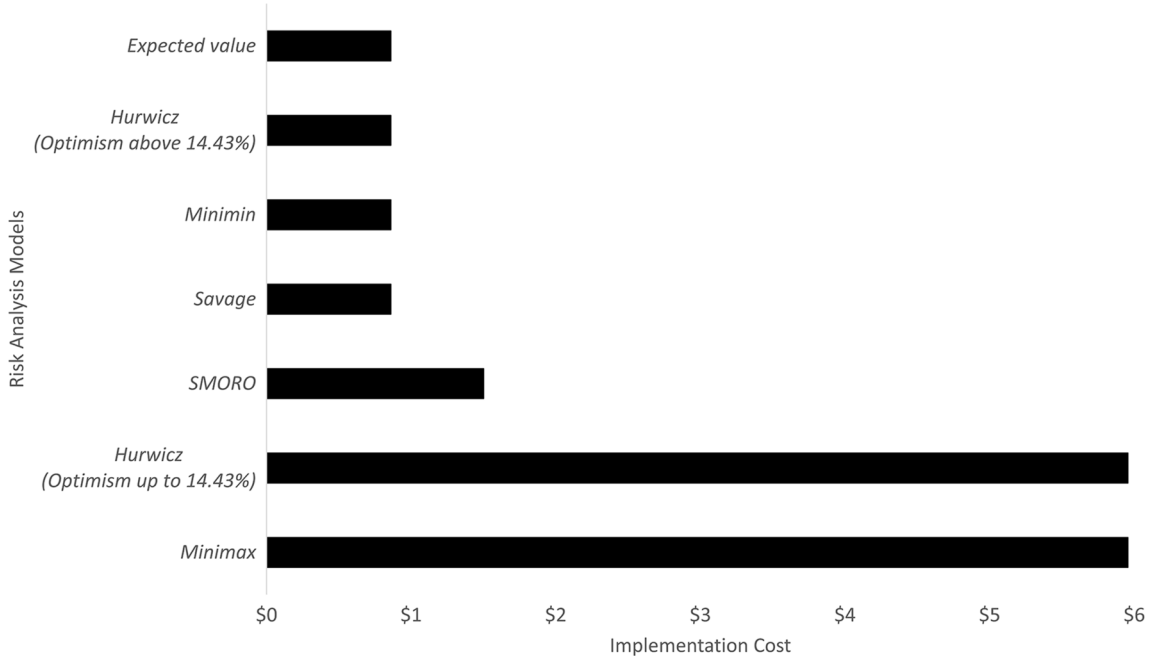

Fig. 7. Implementation cost based on the results of each risk analysis model. Values are in millions of US dollars.

enormous degree of uncertainty in climate change predictions. The six GCMs, analyzed under two greenhouse gas emission pathways (RCPs), provided divergent precipitation trends, demonstrating that the study of climate prediction is highly imprecise.

EQMM was used in conjunction with historical data from a local pluviograph in order to perform statistical downscaling of GCM rainfall data sets. This method proved to be capable of correcting the statistical biases present in the GCM data. In addition, the method has low computational demand, making its use more feasible than dynamic downscaling, which involves significant processing effort that often making its application nonviable.

Quantification of the implementation costs of the urban drainage systems showed how these costs can vary widely depending on the IDF curve selected for their designs. In this context, the proposed decision-making tool appears to be an excellent tool to assist in choosing scenarios that can be adopted to yield a robust urban drainage system design.

Initially, there were 12 possible GCM/RCP scenarios (six GCMs under two future emission pathways—RCP 4.5 and RCP 8.5) to be assessed. There was also a baseline scenario, which was based on the official IDF equation from Fortaleza, making a total of 13 scenarios to be analyzed and compared. Following the application of the six risk analysis models to analyze the costs derived from each GCM/RCP scenario, the number of feasible GCM/RCP scenarios was reduced to three. Two of them presented lower precipitation intensities than the baseline scenario, and only one GCM/RCP scenario showed a considerable increase in rainfall intensity in the city of Fortaleza. Although SMORO was the only risk analysis model that combined scenario and multiobjective optimization, it is important to mention that there are other similar risk analysis models that can be used for future modeling (e.g. Kasprzyk et al. 2013; Mortazavi-Naeini et al. 2015; Eker and Kwakkel 2018) but were not used in this study.

A designer willing to be more conservative should use the equation derived from the CESM1-CAM5/RCP 8.5 scenario, which, although it yielded the most pessimistic and costly design, would yield a more effective design for drainage and flood minimization. By adopting a more optimistic stance—for example, the CANESM2/RCP 4.5 or the BCC_CSM1/RCP 4.5 scenario, which yielded a design with low implementation costs—the designer would be accepting a greater risk of hazards caused by high-intensity rainfall events. The implementation costs for each scenario based on the risk analysis models are shown in Fig. 7. There was great variation in implementation costs between the less conservative results—expected value, Hurwicz (optimism above 14.43%), minimin, Savage, and SMORO—and the most conservative results—Hurwicz (optimism above 14.43%) and minimax. This shows that the set of possible scenarios can vary widely depending on the decision maker's degree of optimism/pessimism. The use of a wider range of scenarios can be of great help, especially for municipal planners and engineers, because it minimizes the risks and uncertainties intrinsic to climate change and enables the selection of a robust, cost-effective, and economically feasible urban drainage system design. It is recommended that other risk analysis models be used in order to make the choice even more reliable in future studies. In addition, it is important to note that if the current methodology is to be used in other locations, a new selection of GCMs and RCPs should be carried out in order to better suit the site studied.

Data Availability Statement

The GCM data were extracted from the Coupled Model Intercomparison Project Phase 5 (CMIP5) website (http://cmip-pcmdi.llnl.gov/cmip5/) in the NetCDF format.

Some or all data, models, or code used during the study were provided by a third party. Direct requests for these materials may be made to the provider as indicated in the Acknowledgments.

Acknowledgments

We acknowledge the World Climate Research Programme's Working Group on Coupled Modeling, which is responsible for coupled model intercomparison project (CMIP), and we thank the climate

modeling groups listed in Table 2 for producing and making available their model output. For CMIP, the US Department of Energy's Program for Climate Model Diagnosis and Intercomparison provides coordinating support and led the development of software infrastructure in partnership with the Global Organization for Earth System Science Portals. Author Marcos Abilio Medeiros de Saboia gratefully acknowledges the financial support provided by the government of the state of Ceará, Brazil.

References

Anderson, M. L., Z.-Q. Chen, M. L. Kavvas, and A. Feldman. 2002. "Coupling HEC-HMS with atmospheric models for prediction of watershed runoff." *J. Hydrol. Eng.* 7 (4): 312–318. https://doi.org/10.1061/(ASCE)1084-0699(2002)7:4(312).

Andrade, E. L. 1989. *Introdução à pesquisa operacional: Métodos e técnicas para análise de decisão*, 377. Rio de Janeiro, Brazil: Livros Técnicos e Científicos.

Andrews, T., J. M. Gregory, and M. J. Webb. 2015. "The dependence of radiative forcing and feedback on evolving patterns of surface temperature change in climate models." *J. Clim.* 28 (4): 1630–1648. https://doi.org/10.1175/JCLI-D-14-00545.1.

Bekman, O. R., and P. L. O. Costa Neto. 1980. *Análise estatística da decisão*. São Paulo, Brazil: Edgard Blucher.

Caixa Econômica Federal. 2020. "SINAPI-Sistema Nacional de Pesquisa de Custos e Índices da Construção Civil." Accessed February 9, 2020. http://www.caixa.gov.br/site/paginas/downloads.aspx.

Chu, X., and A. Steinman. 2009. "Event and continuous hydrologic modeling with HEC-HMS." *J. Irrig. Drain. Eng.* 135 (1): 119–124. https://doi.org/10.1061/(ASCE)0733-9437(2009)135:1(119).

Climate Changes in Australia. 2019. "Greenhouse gas scenarios." Accessed June 28, 2019. https://www.climatechangeinaustralia.gov.au/en/climate-campus/modelling-and-projections/projecting-future-climate/greenhouse-gas-scenarios/.

De Silva, M. M. G. T., S. B. Weerakoon, and S. Herath. 2014. "Modeling of event and continuous flow hydrographs with HEC–HMS: Case study in the Kelani River basin, Sri Lanka." *J. Hydrol. Eng.* 19 (4): 800–806. https://doi.org/10.1061/(ASCE)HE.1943-5584.0000846.

Eker, S., and J. H. Kwakkel. 2018. "Including robustness considerations in the search phase of many-objective robust decision making." *Environ. Modell. Software* 105 (2018): 201–216. https://doi.org/10.1016/j.envsoft.2018.03.029.

Espinet, X., A. Schweikert, and P. Chinowsky. 2017. "Robust prioritization framework for transport infrastructure adaptation investments under uncertainty of climate change." *J. Risk Uncertainty Eng. Syst. Part A: Civ. Eng.* 3 (1): E4015001. https://doi.org/10.1061/AJRUA6.0000852.

Fischer, E. M., and R. Knutti. 2015. "Anthropogenic contribution to global occurrence of heavy-precipitation and high-temperature extremes." *Nat. Clim. Change* 5 (6): 560–564. https://doi.org/10.1038/nclimate2617.

Green, D. 2016. "The spatial distribution of extreme climate events, another climate inequity for the world's most vulnerable people." *Environ. Res. Lett.* 11 (9): 091002. https://doi.org/10.1088/1748-9326/11/9/091002.

Guo, Y. P. 2006. "Updating rainfall IDF relationships to maintain urban drainage design standards." *J. Hydrol. Eng.* 11 (5): 506–509. https://doi.org/10.1061/(ASCE)1084-0699(2006)11:5(506).

Harrington, L. J., D. J. Frame, E. M. Fischer, E. Hawkins, M. Joshi, and C. D. Jones. 2016. "Poorest countries experience earlier anthropogenic emergence of daily temperature extremes." *Environ. Res. Lett.* 11 (5): 055007. https://doi.org/10.1088/1748-9326/11/5/055007.

Hassanzadeh, E., A. Nazemi, and A. Elshorbagy. 2014. "Quantile-based downscaling of precipitation using genetic programming: Application to IDF curves in Saskatoon." *J. Hydrol. Eng.* 19 (5): 943–955. https://doi.org/10.1061/(ASCE)HE.1943-5584.0000854.

Herman, J. D., P. M. Reed, H. B. Zeff, and G. W. Characklis. 2015. "How should robustness be defined for water systems planning under change?" *J. Water Resour. Plann. Manage.* 141 (10): 04015012. https://doi.org/10.1061/(ASCE)WR.1943-5452.0000509.

IPCC (Intergovernmental Panel on Climate Change). 2007. *Climate change 2007: Impacts, adaptation and vulnerability.* Geneva: IPCC.

IPCC (Intergovernmental Panel on Climate Change). 2012. *Managing the risks of extreme events and disasters to advance climate change adaptation*. A Special Rep. of WG I and II. Cambridge, UK: Cambridge University Press.

IPCC (Intergovernmental Panel on Climate Change). 2014. *Climate change 2014: Synthesis report—Contribution of working groups I, II and III to the fifth assessment report of the intergovernmental panel on climate change*. Edited by Core Writing Team, R. K. Pachauri, and L. A. Meyer, 151. Geneva: IPCC.

Kang, D., and K. Lansey. 2013. "Scenario-based robust optimization of regional water and wastewater infrastructure." *J. Water Resour. Plann. Manage.* 139 (3): 325–338. https://doi.org/10.1061/(ASCE)WR.1943-5452.0000236.

Kasprzyk, J. R., S. Nataraj, P. M. Reed, and R. J. Lempert. 2013. "Many objective robust decision making for complex environmental systems undergoing change." *Environ. Modell. Software* 42 (Apr): 55–71. https://doi.org/10.1016/j.envsoft.2012.12.007.

Kassa, A. M. 2017. "Application of decision making with uncertainty techniques: A case of production volume of maize in Ethiopia." *Int. J. Qual. Res.* 11 (2): 331–344. https://doi.org/10.18421/IJQR11.02-06.

Khodakivskyia, O., Y. Khodakivskaa, O. Kuzmenkob, M. Shcherbynaa, and O. Kolesnichenko. 2019. "Improvement of the railway transport system by increasing the level of goal-oriented activity." *Procedia Comput. Sci.* 149 (2019): 415–421. https://doi.org/10.1016/j.procs.2019.01.156.

Kim, H. G., D. K. Lee, C. Park, S. Kil, Y. Son, and J. H. Park. 2015. "Evaluating landslide hazards using RCP 4.5 and 8.5 scenarios." *Environ. Earth Sci.* 73 (3): 1385–1400. https://doi.org/10.1007/s12665-014-3775-7.

Lau, H. C. W., Z. Jiang, W. H. Ip, and D. Wang. 2010. "A credibility-based fuzzy location model with Hurwicz criteria for the design of distribution systems in B2C e-commerce." *Comput. Ind. Eng.* 59 (4): 873–886. https://doi.org/10.1016/j.cie.2010.08.018.

Li, H., J. Sheffield, and E. F. Wood. 2010. "Bias correction of monthly precipitation and temperature fields from intergovernmental panel on climate change AR4 models using equidistant quantile matching." *J. Geophys. Res.* 115 (D10): D10101. https://doi.org/10.1029/2009JD012882.

Mailhot, A., and S. Duchesne. 2010. "Design criteria of urban drainage infrastructures under climate change." *J. Water Resour. Plann. Manage.* 136 (2): 201–208. https://doi.org/10.1061/(ASCE)WR.1943-5452.0000023.

Maimone, M., S. Malter, J. Rockwell, and V. Raj. 2019. "Transforming global climate model precipitation output for use in urban stormwater applications." *J. Water Resour. Plann. Manage.* 145 (6): 04019021. https://doi.org/10.1061/(ASCE)WR.1943-5452.0001071.

Marengo, J. A., R. R. Torres, and L. M. Alves. 2017. "Drought in northeast Brazil—Past, present, and future." *Theor. Appl. Climatol.* 129 (3–4): 1189–1200. https://doi.org/10.1007/s00704-016-1840-8.

Maurer, E. P., and H. G. Hidalgo. 2008. "Utility of daily vs. monthly large-scale climate data: An intercomparison of two statistical downscaling methods." *Hydrol. Earth Syst. Sci.* 12: 551–563. https://doi.org/10.5194/hess-12-551-2008.

Maurer, E. P., G. Kayser, L. Doyle, and A. W. Wood. 2017. "Adjusting flood peak frequency changes to account for climate change impacts in the western United States." *J. Water Resour. Plann. Manage.* 144 (3): 05017025. https://doi.org/10.1061/(ASCE)WR.1943-5452.0000903.

Mavromatidis, G., K. Orehounig, and J. Carmeliet. 2018. "Comparison of alternative decision-making criteria in a two-stage stochastic program for the design of distributed energy systems under uncertainty." *Energy* 156 (Aug): 709–724. https://doi.org/10.1016/j.energy.2018.05.081.

Mirhosseini, G., P. Srivastava, and L. Stefanova. 2013. "The impact of climate change on rainfall intensity–duration–frequency (IDF) curves in Alabama." Supplement, *Reg. Environ. Change* 13 (S1): 25–33. https://doi.org/10.1007/s10113-012-0375-5.

Mishra, V., A. R. Ganguly, B. Nijssen, and D. P. Lettenmaier. 2015. "Changes in observed climate extremes in global urban areas." *Environ. Res. Lett.* 10 (2): 024005. https://doi.org/10.1088/1748-9326/10/2/024005.

Mortazavi-Naeini, M., G. Kuczera, A. S. Kiem, L. Cui, B. Henley, B. Berghout, and E. Turner. 2015. "Robust optimization to secure urban

bulk water supply against extreme drought and uncertain climate change." *Environ. Modell. Software* 69 (2015): 437–451. https://doi.org/10.1016/j.envsoft.2015.02.021.

Mota, S. 2012. *Introdução à engenharia ambiental*. 5th ed. Rio de Janeiro: Associação Brasileira de Engenharia Sanitária e Ambiental.

Municipal Secretariat of Urbanism and Environment. 2013. "Diagnosis of drainage conditions of the municipality of Fortaleza." Accessed February 23, 2016. http://www.fortaleza.ce.gov.br/sites/default/files/drenagem_situacao_de_fortaleza.pdf.

Myhre, G., O. Boucher, F. M. Bréon, P. Forster, and D. Shindell. 2015. "Declining uncertainty in transient climate response as CO_2 forcing dominates future climate change." *Nat. Geosci.* 8 (3): 181–185. https://doi.org/10.1038/ngeo2371.

Phillip, R. 2011. *Kit de Treinamento SWITCH: Gestão integrada das águas na cidade do futuro. Módulo 4. Manejo de águas pluviais: Explorando opções*. 1st ed., 54. São Paulo, Brazil: ICLEI Brazil.

Phillip, R., B. Anton, and P. V. D. Steen. 2011. *Kit de Treinamento SWITCH: Gestão integrada das águas na cidade do futuro. Módulo 1. Planejamento estratégico: Preparando-se para o futuro*. 1st ed., 53. São Paulo, Brazil: ICLEI Brazil.

Prein, A. F., R. M. Rasmussen, K. Ikeda, C. Liu, M. P. Clark, and G. J. Holland. 2017. "The future intensification of hourly precipitation extremes." *Nat. Clim. Change* 7 (1): 48–52. https://doi.org/10.1038/nclimate3168.

Ragno, E., A. AghaKouchak, C. A. Love, L. Cheng, F. Vahedifard, and C. H. R. Lima. 2018. "Quantifying changes in future intensity-duration-frequency curves using multimodel ensemble simulations." *Water Resour. Res.* 54 (3): 1751–1764. https://doi.org/10.1002/2017WR021975.

Sarhadi, A., and E. D. Soulis. 2017. "Time-varying extreme rainfall intensity-duration-frequency curves in a changing climate." *Geophys. Res. Lett.* 44 (5): 2454–2463. https://doi.org/10.1002/2016GL072201.

Schardong, A., R. K. Srivastav, and S. P. Simonovic. 2015. *Computerized tool for the development of intensity-duration-frequency curves under a changing climate—User's manual*. London: Dept. of Civil and Environmental Engineering, Western Univ.

Scharffenberg, W. A. 2013. *Hydrologic modeling system HEC-HMS: User's manual*. Davis, CA: US Army Corps of Engineers, Hydrologic Engineering Center.

Semadeni-Davies, A., C. Hernebring, G. Svensson, and L. Gustafsson. 2008. "The impacts of climate change and urbanisation on drainage in Helsingborg, Sweden: Combined sewer system." *J. Hydrol.* 350 (1–2): 100–113. https://doi.org/10.1016/j.jhydrol.2007.05.028.

Silveira, C. S., F. A. Souza Filho, A. A. Costa, and S. L. Cabral. 2013. "Avaliação de desempenho dos modelos do cmip5 quanto à representação dos padrões de variação da precipitação no século xx sobre a região nordeste do brasil, amazônia e bacia da prata e análise das projeções para o cenário rcp8. 5." *Rev. Bras. Meteorol.* 28 (3): 317–330. https://doi.org/10.1590/S0102-77862013000300008.

Silveira, C. S., F. A. Souza Filho, E. S. P. R. Martins, J. L. Oliveira, A. C. Costa, M. T. Nobrega, and R. F. V. Silva. 2016. "Mudanças climáticas na bacia do rio São Francisco: Uma análise para precipitação e temperature." *Rev. Bras. Recursos Hídricos* 21 (2): 416–428. https://doi.org/10.21168/rbrh.v21n2.p416-428.

Simonovic, S. P., A. Schardong, and D. Sandink. 2016. "Mapping extreme rainfall statistics for Canada under climate change using updated intensity-duration-frequency curves." *J. Water Resour. Plann. Manage.* 143 (3): 04016078. https://doi.org/10.1061/(ASCE)WR.1943-5452.0000725.

Srivastav, R. K., A. Schardong, P. Slobodan, and S. P. Simonovic. 2014. "Equidistance quantile matching method for updating IDF curves under climate change." *Water Resour. Manage.* 28 (9): 2539–2562. https://doi.org/10.1007/s11269-014-0626-y.

Steenhuis, T. S., M. Winchell, J. Rossing, J. A. Zollweg, and M. F. Walters. 1995. "SCS runoff equation revisited for variable-source runoff areas." *J. Irrig. Drain. Eng.* 121 (3): 234–238. https://doi.org/10.1061/(ASCE)0733-9437(1995)121:3(234).

Thakali, R., A. Kalra, and S. Ahmad. 2016. "Understanding the effects of climate change on urban stormwater infrastructures in the Las Vegas Valley." *Hydrology* 3 (4): 34. https://doi.org/10.3390/hydrology3040034.

Tucci, C. E. M. 1993. *Hidrologia, ciência e aplicação*, 4th ed. Porto Alegre, Brazil: Editora da Universidade.

USDA. 1986. *Urban hydrology for small watersheds*. Technical Release No. 55. Washington, DC: USDA Soil Conservation Service.

Van Vuuren, D. P., J. Edmonds, M. Kainuma, K. Riahi, A. Thomson, K. Hibbard, and T. Masui. 2011. "The representative concentration pathways: An overview." *Clim. Change* 109 (1–2): 5. https://doi.org/10.1007/s10584-011-0148-z.

Williams, J. R., N. Kannan, X. Wang, C. Santhi, and J. G. Arnold. 2012. "Evolution of the SCS runoff curve number method and its application to continuous runoff simulation." *J. Hydrol. Eng.* 17 (11): 1221–1229. https://doi.org/10.1061/(ASCE)HE.1943-5584.0000529.

Yu, B. 2012. "Validation of SCS method for runoff estimation." *J. Hydrol. Eng.* 17 (11): 1158–1163. https://doi.org/10.1061/(ASCE)HE.1943-5584.0000484.